Tumor Microenvironment Alters Chemoresistance of Hepatocellular Carcinoma Through CYP3A4 Metabolic Activity

Alican Özkan[1,11*], Danielle L. Stolley[2], Erik N. K. Cressman[3], Matthew McMillin[4,5], Sharon DeMorrow[4,5,6], Thomas E. Yankeelov[2,7,8,9,10], Marissa Nichole Rylander[1,2,7]

[1] Department of Mechanical Engineering, The University of Texas, Austin, TX, 78712, United States
[2] Department of Biomedical Engineering, The University of Texas, Austin, TX, 78712, United States
[3] Department of Interventional Radiology, The University of Texas MD Anderson Cancer Center, Houston, TX, 77030. United States
[4] Department of Internal Medicine, Dell Medical School, The University of Texas at Austin, Austin, TX, United States
[5] Central Texas Veterans Health Care System, Temple, TX, United States
[6] Division of Pharmacology and Toxicology, College of Pharmacy, The University of Texas at Austin, Austin, TX 78712, United States
[7] Oden Institute for Computational Engineering and Sciences, The University of Texas, Austin, TX, 78712, United States
[8] Departments of Diagnostic Medicine, The University of Texas, Austin, TX, 78712, United States
[9] Department of Oncology, The University of Texas, Austin, TX, 78712, United States
[10] Livestrong Cancer Institutes, Dell Medical School, The University of Texas, Austin, TX, 78712, United States
[11] Current address: Wyss Institute for Biologically Inspired Engineering at Harvard University, Boston, MA, 02115, United States.

*** Correspondence:** Alican Özkan, alican.ozkan@wyss.harvard.edu

Keywords: Hepatocellular Carcinoma, Cirrhosis, Desmoplasia, Chemoresistance, Hypoxia, 3D cell culture, CYP Metabolism, Tissue Engineering, Drug Metabolization

Abstract

Variations in tumor biology from patient to patient combined with the low overall survival rate of hepatocellular carcinoma (HCC) present significant clinical challenges. During the progression of chronic liver diseases from inflammation to the development of HCC, microenvironmental properties, including tissue stiffness and oxygen concentration, change over time. This can potentially impact drug metabolism and subsequent therapy response to commonly utilized therapeutics, such as doxorubicin, multi-kinase inhibitors (e.g., sorafenib), and other drugs, including immunotherapies. In this study, we utilized four common HCC cell lines embedded in 3D collagen type-I gels of varying stiffnesses to mimic normal and cirrhotic livers with environmental oxygen regulation to quantify the impact of these microenvironmental factors on HCC chemoresistance. In general, we found that HCC cells with higher baseline levels of cytochrome p450-3A4 (CYP3A4) enzyme expression, HepG2 and C3Asub28, exhibited a cirrhosis-dependent increase in doxorubicin chemoresistance. Under the same conditions, HCC cell lines with lower CYP3A4 expression, HuH-7 and Hep3B2, showed a decrease in doxorubicin chemoresistance in response to an increase in microenvironmental stiffness. This differential therapeutic response was correlated with the regulation of CYP3A4 expression levels under the influence of stiffness and oxygen variation. In all tested HCC cell lines, the addition of sorafenib lowered the required doxorubicin dose to induce significant levels of cell death, demonstrating its

potential to help reduce systemic doxorubicin toxicity when used in combination. These results suggest that patient-specific tumor microenvironmental factors, including tissue stiffness, hypoxia, and CYP3A4 activity levels, may need to be considered for more effective use of chemotherapeutics in HCC patients.

1 Introduction

Cancer is the second-highest cause of mortality in the United States, lagging just slightly behind cardiovascular disease in 2019 [1]. Among all cancer types, hepatocellular carcinoma (HCC) has the second-lowest 5-year survival rate (17.7%) and has shown the highest increase in mortality among all cancers over the past seven years [2,3]. Complicating treatment, HCC is commonly diagnosed at an intermediate or an advanced stage and often occurs secondary to underlying chronic liver disease and cirrhosis [4]. The prognosis is poor as treatment options are limited by compromised liver function due to underlying disease. Despite screening efforts for at-risk patients, most are not surgical candidates for partial resection, and the availability of full liver transplantation is very low relative to the need[5].

These issues mean that systemic and localized drug-based therapies play a significant role in current standard therapy for HCC. Despite these therapeutic interventions, the survival rate for HCC remains low, partially attributed to the variable efficacy of current treatment methods based on underlying factors [6–8]. As such, stratifying patients for the most effective treatment is critical because of three factors; the degree of tumor burden, the degree of liver dysfunction, and highly variable treatment efficacy between patients [9]. For example, the tyrosine kinase inhibitor sorafenib has shown modest success in selected patients as a systemic treatment [10], but effectiveness is tempered by poor tolerance of the drug in many instances[9]. Localized delivery of drugs through transarterial chemoembolization (TACE) combines delivery of drugs such as doxorubicin with embolization to promote localized ischemia and hypoxia. TACE blocks the arterial blood supply of a tumor through particulate or viscous liquid agents such as degradable starch microspheres, drug-eluting beads, or ethiodized oil. This is a well-established technique that allows a high local dose while simultaneously increasing the residence of chemotherapeutic drugs in the target area, cutting off the supply of nutrients, and also limiting exposure and toxicity for the rest of the body [11]. This has emerged as the standard of care for intermediate-stage HCC. However, tumor cells in the hypoxic environment may undergo phenotypic adaptations that aid survival. Such changes may account for the high rate of persistent, viable tumor cells observed after TACE in previous studies [12]. Therefore, while a substantial survival benefit can be realized, there is still much room for improvement and understanding of the changes that occur in the tumor cells during embolization[6–8].

It is well established that many of the difficulties in treating HCC may stem from the numerous tumor microenvironment (TME) changes that occur in underlying chronic liver disease and the rapid progression of HCC. The modulation of the TME has been shown to impact drug metabolism significantly and is thought to be a major contributor to the known differential response of patients to chemotherapy [13,14]. Furthermore, induction of hypoxia in the TME due to stiffening of the extracellular matrix (ECM) and embolization during treatment can alter the chemoresistance of the tumor cells, further impacting the treatment efficiency in intermediate and advanced stage HCC [15–17]. The modulation of response and the individual impact of these TME features have yet to be fully characterized in a three-dimensional (3D) HCC-TME model.

The increase in microenvironmental stiffness resulting from fibrosis, usually culminating in cirrhosis, is a hallmark of most chronic liver diseases and is observed in 80-90% of HCC patients [4]. The most notable hallmark of liver cirrhosis that impacts cellular and tissue function is increased collagen

This is a provisional file, not the final typeset article

87 deposition from activated hepatic stellate cells, increasing the stiffness and compression modulus of
88 liver tissue [18]. Similarly, the progression of HCC is marked by further localized stiffening. This
89 desmoplastic reaction is attributed to further differentiation of liver stellate cells into myofibroblasts
90 [18], resulting in additional deposition of collagen[19]. This stiffening of the ECM, in conjunction with high
91 tumor cell density, further reduces local oxygen and nutrient diffusion. Limited oxygen availability has
92 been shown to alter the outcomes of the chemotherapeutic treatments by affecting the drug transporters'
93 p-glycoprotein (MDR1, multidrug resistance 1), drug targets (topoisomerase II), or by initiating drug-
94 induced apoptosis [20]. Subsequent alterations in the cancer cells' response to chemotherapy can occur
95 through modulation of chemoresistance markers and hepatocyte metabolic enzymes such as
96 cytochrome P450 (CYP450), primarily the CYP3A4 subgroup [21]. Thus CYP3A4 expression can
97 potentially serve as an indicator for predicting chemotherapeutic response [22]. This highlights a potential
98 mechanism of differential tumor chemoresistance through the modulation of CYP3A4 under different
99 microenvironmental conditions.

100 Numerous *in vitro* models have been used to study the impact of TME modulation on HCC
101 treatment response. Two-dimensional (2D) cell monolayers have documented an increase in HepG2
102 cell survival following exposure to doxorubicin during hypoxia compared to normoxic conditions [23].
103 However, traditional 2D cell culture models do not allow for adequate representation of the
104 physiological diffusion and associated transport barriers found in the 3D extracellular
105 microenvironment, limiting clinical translation. Tumor spheroid models have been utilized as a more
106 representative system for assessing HCC drug response in direct cell-cell contacts and the subsequent
107 decrease of HCC chemoresistance [24]. However, the lack of ECM in these models severely curtails the
108 study of the interactions with and subsequent tuning of the ECM components of the TME [25].

109 Previous efforts that address the importance of ECM microenvironmental properties on the
110 chemotherapeutic response, employ tunable hydrogels models, composed of cells cultured in ECMs of
111 collagen, fibrin, alginate, and Matrigel™. These models have been used to investigate the ECM's role
112 in *in vitro* studies of chemotherapy response, drug transport, cell invasion, and differentiation [25,26].
113 Culturing different breast cancer cell lines in an alginate hydrogel showed doxorubicin
114 chemoresistance was altered in particular phenotypes when ECM stiffness was increased [27]. With
115 respect to metabolic activity, one study investigated Ifosfamide metabolism by C3A HCC cells with
116 different levels of CYP3A4 expression when cultured in polylactic acid (PLA) [28]. However, this study
117 reported treatment efficacy only with glioblastoma cells and did not explore or discuss the treatment
118 response of liver cells. Another study demonstrated that culturing Caco-2 colorectal cancer cells on the
119 top of a 3D collagen-Matrigel™ blended hydrogel with dynamic flow conditions increased CYP3A4
120 expression drastically compared to 2D monolayers without flow [29]. Similarly, another study showed
121 that the CYP3A4 activity of HepaRG HCC cells increased when cells were cultured in hyaluronan-
122 gelatin or wood-derived nanofibrillar cellulose ECMs relative to 2D monolayer culture [30]. Research
123 has shown culturing U251 and U87 glioblastoma cells in 3D PLA scaffold under hypoxia exhibited
124 higher resistance to doxorubicin and greater production of basic fibroblast growth factor (bFGF) and
125 vascular endothelial growth factor (VEGF)[31]. Furthermore, U87, U251, and SNB19 glioblastoma cells
126 have been shown to be more resistant to temozolomide when cultured in scaffold-free spheroids under
127 hypoxic conditions compared to comparable spheroids under normoxic conditions [32]. Other studies
128 have used native ECM (collagen and fibrin) and non-native polymers (agar, acrylamide, and polylactic
129 acid) to recapitulate 3D breast and hepatic tumor microenvironments. However, these studies did not
130 investigate the regulation of cellular metabolism, including CYP3A4 activity, under different
131 microenvironmental conditions [26,27,33,34]. Recent work extending these efforts has demonstrated
132 significant potential in utilizing collagen tunability to replicate native microenvironment properties

133 (pH, stiffness, fiber properties, and porosity) [35,36], demonstrating promise in replicating physiological
134 TME to investigate the modulation of CYP3A4 activity and chemoresistance.

135 In this study, we utilized a collagen type I hydrogel to investigate the influence of ECM stiffness,
136 oxygen concentration, cell type, and the availability of a 3D microenvironment (2D vs. 3D) on drug
137 metabolism and response to two common chemotherapeutic agents, doxorubicin and sorafenib, both
138 individually and in combination. We used four established HCC cell lines (HepG2, C3Asub28, HuH-
139 7, and Hep3B2), which present with different basal metabolic profiles of CYP3A4 expression to
140 quantify the impact of modulations of the TME. Our results demonstrate the importance of the
141 contribution of a 3D ECM in drug design and dosing based on the significant differences seen in drug
142 response and metabolism when tumor cells are cultured in 3D collagen type I compared to traditional
143 2D culture. Further, we show that variations in the liver TME, including liver stiffness and hypoxia,
144 results in altered drug metabolism and subsequent drug efficacy. Tissue stiffness, varied by using
145 collagen concentrations comparable to healthy and cirrhotic liver stiffnesses [37], caused an alteration in
146 chemoresistance and drug metabolism. Environmental oxygen regulation to simulate normoxic and
147 hypoxic conditions produces a similarly significant, general effect on both chemoresistance and drug
148 metabolism. However, the TME regulation was not consistent for every cell type investigated, shown
149 in the heterogeneous regulation of cell chemoresistance and drug metabolism in the HCC cell lines.
150 This highlights a potential clinically translational impact of HCC genetic polymorphisms and different
151 etiologies on treatment outcome. Specifically, we identify that the basal cellular CYP3A4 metabolism
152 can be differentially regulated by TME hypoxia and tissue stiffness, thus impacting the efficacy of
153 commonly used HCC therapeutics. This relationship provides a potential explanation of the poor
154 outcomes of drugs in HCC clinical trials and may eventually lead to improve outcomes for HCC
155 patients.

156 **2 Methods**

157 **2.1 Cell Culture**

158 Human hepatocellular carcinoma cell lines HepG2 (HB-8065™, ATCC®, Manassas, VA), HuH-7,
159 Hep3B2.1.7, and HepG2 derived C3A with enhanced expression of CYP3A4 mRNA and CYP3A4-
160 mediated activity (C3Asub28) [38] were used in this study. HuH-7 cells express a mutated form of tumor-
161 suppressive protein p53, leading to an increased half-life and accumulation of the protein in cell nuclei.
162 This has been shown to correlate with increased chemoresistance [39]. Hep3B2.1.7 was used as an
163 example of an HCC tumor with hepatitis B DNA in the genome and subsequent mutations, including
164 partially deleted and suppressed expression of p53. All cells were cultured with DMEM supplemented
165 with 10% heat-inactivated fetal bovine serum (FBS, F4135, Sigma Aldrich, MO) and 1%
166 Penicillin/Streptomycin (P/S, Invitrogen, CA). Normoxic conditions were similarly generated by
167 culturing cells in standard cell culture conditions in a normoxic incubator (21% O_2, 5% CO_2, 37˚C
168 Thermo Fisher Scientific, Rochester, NY, USA). Hypoxic conditions were simulated by placing cells
169 in a sealed incubator (1% O_2, 5% CO_2). All cells were grown to approximately 70% confluence and
170 used within the first eight passages.

171 **2.2 Preparation and Tuning of Collagen**

172 Type I collagen isolated from rat tail tendons (donated by the University of Texas at Austin - Institute
173 for Cellular and Molecular Biology) was used to recapitulate the tissue microenvironment as it is the
174 primary ECM component of human tissue, including the liver [26]. As we have previously published, a
175 stock solution of type I collagen was prepared by dissolving excised rat tail tendons in an HCl solution
176 at a pH of 2.0 for 12 hours at 23˚C [26]. The solution was then centrifuged at 4˚C for 45 minutes at 30000

This is a provisional file, not the final typeset article

177 g, and the supernatant was collected, lyophilized, and stored at -20˚C. The lyophilized collagen was
178 mixed with diluted 0.1% glacial acetic acid, maintained at 4˚C, and vortexed every 24 hours for three
179 days to create a collagen stock solution. Finally, collagen was centrifuged at 4˚C for 10 minutes at 2700
180 rpm to remove air bubbles. Collagen concentrations of 4 and 7 mg/ml were used to replicate normal
181 and cirrhotic liver stiffness, respectively, which we have previously demonstrated to match native liver
182 compression moduli after cells have reached their native morphology [26,37]. Collagen solutions were
183 adjusted to pH 7.4 with 1X DMEM, 10X DMEM (Sigma Aldrich, St. Louis, MO), and 1N NaOH
184 (Fisher Scientific, Pittsburgh, PA.). Following this, the collagen mixture was mixed with the intended
185 HCC cell lines uniformly at a concentration of $1x10^6$ cells/ml. Each suspension was dispensed as 50
186 µL aliquots in 96 well plates and allowed to polymerize. For 2D monolayer samples, identical numbers
187 of cells in 100 µL of media were dispensed into the wells of a 96 well plate. Cell media was changed
188 every two days.

189 **2.3 Confined Compression Test**

190 Cirrhotic stiffening in the TME has been shown to alter the chemoresistance of many cancer cell types
191 [40]. As a result, the mechanical properties of the TME, such as compression modulus, also increase**.** The
192 compression modulus of 3D collagen hydrogels was measured with quasi-steady uniaxial unconfined
193 compression (Instron, Norwood, MA) [26] to ensure there is no significant difference between collagen
194 gels with different HCC cell lines three days after seeding. In the analysis, the hydrogels are assumed
195 to be linear under the deformation conditions, and the slope of the stress-strain curve represents the
196 compression modulus. Hydrogels were prepared as described in the previous section, and 500 µL of
197 hydrogels were placed inside 24 well plates. Polymerized collagen samples were punched (9.53 mm
198 diameter) to remove the concave meniscus at the sample edge. Samples were compressed using a 20
199 mm diameter load cell of a flat steel surface. Load cells (10 N Static Load Cell, 2519-10N) were
200 lowered approximately 2.5 mm away from the flat surface and displaced 2 mm at a rate of 0.0085 mm/s
201 to achieve 0.1% strain/s over the range of 0-20% strain. Stress was calculated from the force response
202 divided by the initial area of collagen sample (71.26 mm^2). All measurements were performed at room
203 temperature (23˚C) and the total duration of each experiment was less than 4 minutes. The data was
204 analyzed using Matlab® (MathWorks, Natick, MA).

205 **2.4 Dosing With Chemotherapeutics**

206 Doxorubicin and sorafenib have been commonly used in ongoing clinical trials for HCC treatment
207 either alone or in combination [41]. Prepared samples were exposed to doxorubicin (D1515, Sigma-
208 Aldrich, St. Louis, MO) with or without sorafenib (HY-10201, MedChemExpress LLC, Monmouth
209 Junction, NJ,) for 24 and 48 h. A broad range (1 nM – 200µM) of doxorubicin concentrations were
210 used to determine the response across the different HCC cell lines. Three different doses of sorafenib
211 were used to replicate previously tested effective concentrations: none (0 µM), standard (11 µM), and
212 high (22 µM) [42]. Samples were washed with warm (37˚C) 1x phosphate buffered saline (PBS) three
213 times to remove the excess drug after the treatment. Cell culture media was used as a negative control.

214 **Measuring** Viability: Cell viability 72 hours after the completion of drug treatment was measured with
215 Cell Titer Blue (G8081, Promega, Fitchburg, WI) cell viability assay to quantify the response of HCC
216 cells to chemotherapeutic treatment under varying TME conditions (such as stiffness and hypoxia).
217 Briefly, cell media was mixed at a ratio of 5:1 with assay solution and incubated at 37˚C for 1 hr. A
218 Cytation 3 plate reader was used to read fluorescence (Ex: 530 nm/Em: 620 nm) of the assay. Findings
219 were normalized to control (cells treated with drug-free media) to obtain percent cell viability. The
220 data gathered from cell viability assays after doxorubicin treatment was fitted using the cftool function
221 of Matlab® (MathWorks, Natick, MA) and half-maximal inhibitory concentration (IC50) value was

222 calculated and reported as chemoresistance indicator. As sorafenib has been used as a prodrug used for
223 angiogenesis treatment, mainly by inhibiting vascular endothelial growth factor (VEGFR), platelet-
224 derived growth factor receptor (PDGFR), and rapidly Accelerated Fibrosarcoma (RAF), but it also has
225 a minor direct cytotoxic side-effect in some instances [15]. For that reason, treatment efficacy of
226 standalone sorafenib and combined treatments were reported as fold viability change compared to
227 untreated control for the two clinically relevant doses used, standard (11 μM), and high (22 μM).
228 Additionally, for combined treatment, the minimum required doxorubicin dose to initiate toxicity was
229 reported. For this analysis, statistical comparison ($p<0.05$) of viability under the tested doses and
230 untreated samples were compared, and the minimum dose was reported.

231 **2.5 CYP3A4 Activity Measurement**

232 Overexpression of CYP3A4 has been shown to decrease the efficacy of chemotherapeutics and is one
233 of the main challenges in the treatment of HCC tumors [22]. To relate the chemotherapeutic response to
234 the metabolic activity of HCC cells under the influence of hypoxia and different stiffnesses, the
235 expression of CYP3A4 was quantified using P450-Glo™ Assay and Screening Systems (V9001,
236 Promega, Madison, WI) in response to different oxygen concentrations, normoxic and hypoxic, and
237 different spatial conditions, 2D, 3D normal, and 3D cirrhotic. HCC cells were cultured in 2D or 3D, as
238 previously described for three days before CYP3A4 measurements to allow cells to reach native
239 morphology [37]. Prepared samples were washed twice with PBS and incubated with 50 μL of CYP3A4
240 substrate Luciferin-IPA (3 μM, dissolved in 1X DMEM). After 1 hour of incubation at 37˚C, 50 μL of
241 Luciferin Detection Reagent was added and pipetted up and down several times to ensure cell lysis.
242 After 20 minutes of incubation at room temperature, cell supernatants were transferred to a 96-well
243 opaque white luminometer plate (white polystyrene; Costar, Corning Incorporated) and luminescence
244 was measured using a Cytation 3 plate reader (BioTek Instruments, Inc., VT). Reagents without cells
245 were included as background controls. Metabolic activities were calculated by subtracting the
246 background luminescence and normalizing to the seeded cell number.

247 **2.6 Statistical Analysis**

248 Two-tailed student's t-test assuming unequal variance was performed in Matlab® (MathWorks, Natick,
249 MA) to compare samples, and a p-value less than 0.05 was considered significant for variation. Data
250 are reported as mean ± standard deviation unless otherwise indicated. All experiments were replicated
251 a minimum of four times.

252 **3 Results**

253 HCC cells were cultured for three days to reach native morphology in a monolayer in a tissue culture
254 plate (2D) or in rat tail-derived collagen type I hydrogels (3D). Cells were treated with doxorubicin
255 with or without sorafenib for 24 or 48 hours. Viability was assessed 72 hours after the end of drug
256 treatment, as described in Figure 1a.

This is a provisional file, not the final typeset article

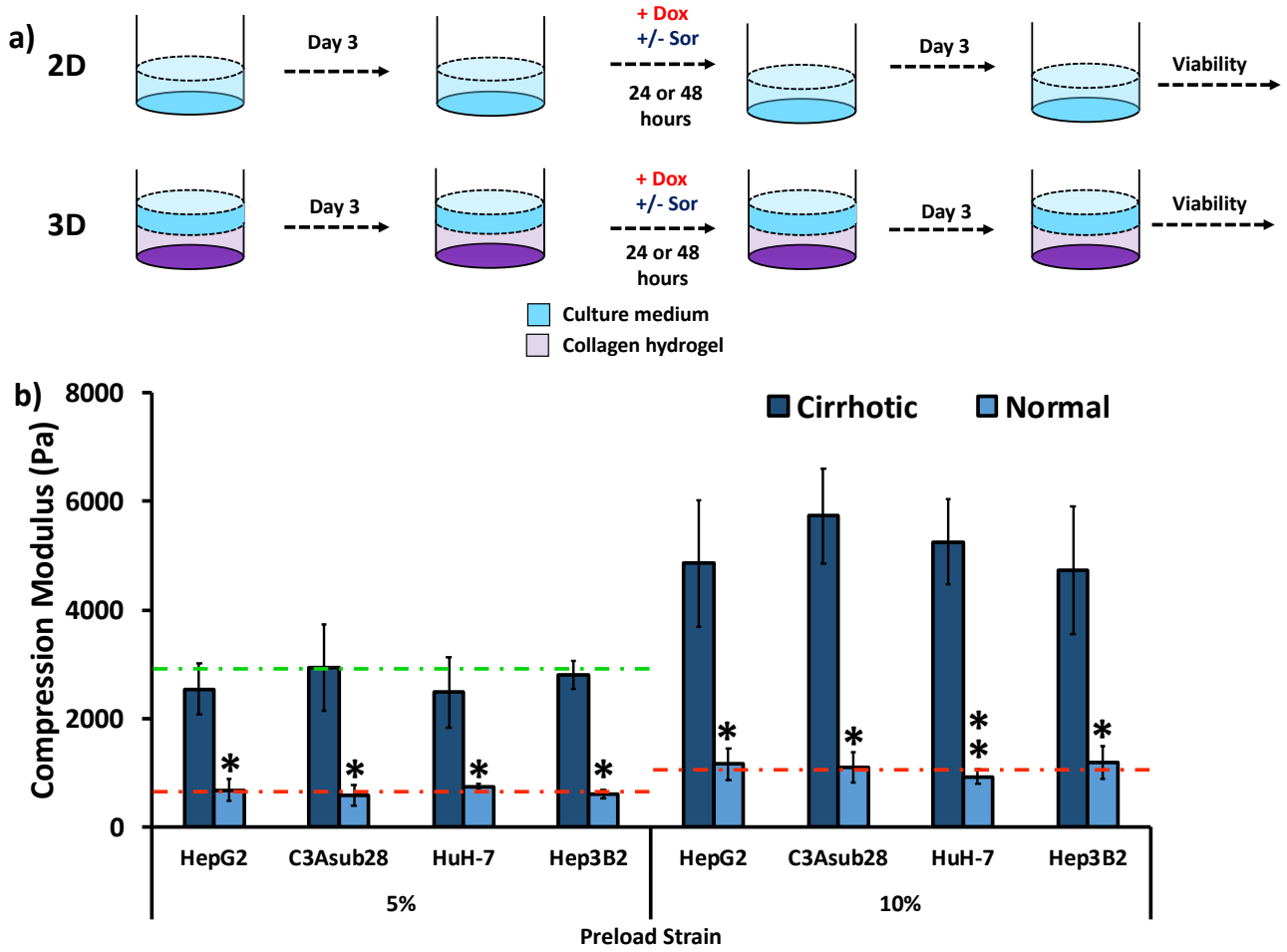

Figure 1: HCC cells cultured in a monolayer or in collagen hydrogels of varying stiffness. **a)** Experimental procedure outline. Cells were allowed to adhere and reach their native morphology before the treatment for 24 or 48 hours. **b)** Compression modulus of the HCC hydrogels with 4 and 7 mg/ml collagen concentrations, which replicate normal and cirrhotic tissues, respectively. The compression modulus did not vary when different HCC cells were cultured in collagen hydrogels. Compression modulus values were significantly different when different collagen concentrations were used to replicate normal and cirrhotic conditions. Dashed lines represent patient compression modulus of healthy (red) and cirrhotic (green) tissues. [43,44]. Selected collagen concentrations replicated native tissues successfully at different preload strains. * $p<0.05$, ** $p<0.01$.

3.1 Native 3D Microenvironment Compression Modulus

Hepatocytes uniformly embedded inside rat tail-derived collagen type I hydrogels were allowed to reach their native morphology for three days. Afterwards, stiffness of the collagen hydrogels was quantified using a uniaxial compression test with 5% and 10% preload strains as presented in Figure 1b to determine any potential impact of different HCC cell lines on collagen stiffness. Our results demonstrate that increasing collagen concentration significantly elevated the compression modulus of the collagen gels ($p<0.05$). However, we found no significant difference between compression modulus between collagen hydrogels with the different HCC cell lines over the timeframe considered. Collagen hydrogels at 4 mg/ml concentration produce a compression modulus comparable to tissue in a normal hepatic microenvironment, which has been reported to be at 0.64 ± 0.08 kPa and 1.08 ± 0.16 kPa for 5% and 10% preload strains, respectively [43]. At 4 mg/ml collagen concentration, the average

compression modulus was found to be 0.66 ± 0.07 kPa and 0.11 ± 0.01 kPa for 5% and 10% preload strains, respectively. Likewise, at 7 mg/ml collagen concentration, collagen hydrogels achieved a compression modulus comparable to a human hepatic tumor microenvironment, which has been reported to be 3 kPa under 5% preload strain [44]. The significant difference ($p<0.05$) of compression moduli between 7 mg/ml and 4 mg/ml collagen hydrogels showed we could replicate the microenvironment stiffness using these collagen properties. In our findings, using a 7 mg/ml collagen concentration, the average compression modulus was found to be 2.70 ± 0.22 kPa for 5% preload strain. The reported collagen compression moduli for this study are also consistent with our previously reported collagen compression modulus values[26]. In the same study, we also showed that collagen concentration does not alter the diffusivity of solutes, thereby demonstrating that differential response to chemotherapy is not likely due to physical diffusion differences of the collagen concentrations [26].

3.2 Matrix Stiffness and Hypoxia Modulate Doxorubicin Chemoresistance in Hepatic 2D and 3D Cultures

HCC cell viability in response to doxorubicin treatment under different microenvironmental conditions was measured. The resulting half-maximal inhibitory concentrations (IC50) of doxorubicin was quantified for HepG2, C3Asub28, HuH-7, and Hep3B2 cells in 2D monolayers and 3D collagen hydrogels at 4 mg/mL (3D-normal) or 7 mg/mL (3D-cirrhotic) to demonstrate the impact of the tumor structural microenvironment on the hepatic response to this drug. Furthermore, the impact of oxygen concentration was quantified through the environmental regulation of normoxic (21% O_2) and hypoxic (1% O_2) conditions for 2D and 3D cultures. The IC50 values of doxorubicin after 24-hour treatments are summarized in Figure 2. IC50 values for 48-hour treatment durations can be found in Fig S-I as minimal changes to IC50 values were observed with the increased treatment duration. Overall, we demonstrated that the IC50 values of doxorubicin against C3Asub28 cells were the highest compared to other HCC cells, in agreeance with the sub-strain's increased drug metabolism through CYP3A4.

This is a provisional file, not the final typeset article

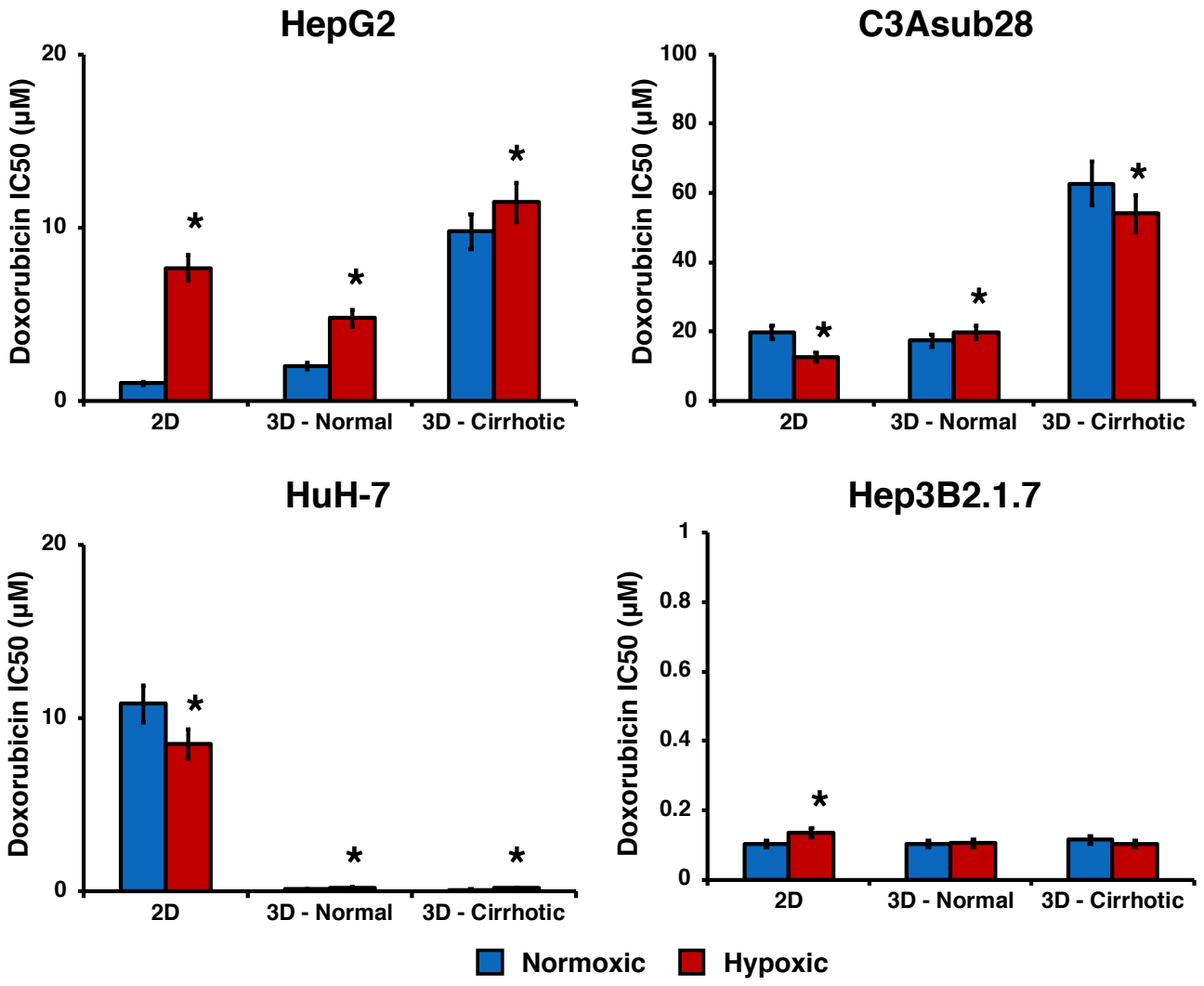

Figure 2: Half-maximal inhibitory concentrations (IC50) values of doxorubicin against HCC cells in different microenvironments. HCC cells have stiffness and oxygen-dependent resistance/sensitivity to 24-hour doxorubicin treatment. Cirrhosis and hypoxia altered IC50 findings differently among the HCC cell lines. 3D-normal: 4 mg/ml collagen gel, 3D-Cirrhosis: 7 mg/ml collagen gel. Statistical significance was compared to normoxic conditions. *$p<0.05$.

3.3 Comparison of Doxorubicin IC50 for 2D vs. 3D Culture under Normoxic Conditions

Studies have demonstrated that 3D matrix stiffness plays an important role in modulation of the cellular response to chemotherapeutics in some cancer cell lines, providing a significantly different response compared to standard 2D culture methods [27,45]. However, few groups demonstrate the variation of IC50 values of doxorubicin between standard 2D-monolayer and 3D culture under varying microenvironmental conditions. In the context of the 3D microenvironment, we were able to determine the influence of normal liver stiffness (4 mg/mL collagen) under normoxic conditions (21% O_2) compared to 2D-normoxic monolayers as calculated by the fold change in chemoresistance due to the presence of the 3D microenvironment. In general, we demonstrate that IC50 values of doxorubicin against HepG2 increased in 3D compared to 2D but did not change for the C3Asub28 cell line. In contrast, 3D culture decreased IC50 values of doxorubicin for HuH-7 and Hep3B2 cell lines compared to 2D monolayers.

320 We observed that IC50 of HepG2 cells after a 24-hour doxorubicin treatment was 3.09-fold higher in
321 the 3D normal-normoxic environment (IC50 = 1.13 μM) compared to the 2D-normoxic (IC50 = 3.48
322 μM). The IC50 of doxorubicin against C3Asub28 cells was consistently the highest, but it was the only
323 cell line that did not lead to a significant change in IC50 of doxorubicin in response to the 3D normal-
324 normoxic compared to 2D-normoxic. The efficacy of doxorubicin on HuH-7 cells cultured in 3D
325 normal-normoxic microenvironment was higher than the HepG2 and C3Asub28 phenotypes. Overall,
326 we observed that the IC50 of doxorubicin against HuH-7 cells was lower ($p<0.05$) in 3D normal-
327 normoxic compared to 2D-normoxic by 62.61-fold. Conversely, IC50 values of doxorubicin against
328 Hep3B2 cells were the lowest overall and significantly decreased 4.02-fold 3D normal-normoxic
329 compared to 2D-normoxic.

330 3.4 The Influence of Microenvironmental Stiffness on Doxorubicin Chemoresistance under 331 Normoxic Conditions

332 To isolate the impact that microenvironmental stiffness plays in the regulation of chemoresistance of
333 different HCC cell lines, we analyzed the impact that the shift from normal (4 mg/mL) to cirrhotic (7
334 mg/mL) collagen concentration has on doxorubicin IC50 values under normoxic conditions for a 24-
335 hour treatment duration. Overall, we found that the increase in microenvironmental stiffness, modeled
336 by the higher collagen concentration, increased the IC50 values of doxorubicin against the HCC cell
337 lines, HepG2 and C3Asub28, that had a higher basal chemoresistance to doxorubicin. Variations in
338 fold changes for 24-hour treatment were reported in Figure S-II. 48-hour treatment duration resulted
339 in marginal differences in IC50 values compared to 24-hour treatment duration (Figure S-III). The
340 IC50 of doxorubicin against HepG2 (3.24-fold) and C3Asub28 (2.22-fold) cells cultured in 3D
341 cirrhotic-normoxic conditions increased compared to cells cultured in 3D normal-normoxic conditions.
342 However, for both HuH-7 and Hep3B2.17, we did not see any significant difference in IC50 values of
343 doxorubicin against these cells ($p>0.05$), between 3D normal-normoxic and 3D cirrhotic-normoxic
344 conditions.

345 3.5 Influence of Hypoxia on Doxorubicin Chemoresistance

346 Oxygen concentration in HCC liver tumors can change due to reduced blood flow, increased
347 cell density, and environmental stiffening [17,23]. This has been shown to alter both the proliferation rate
348 and chemoresistance of tumor cells. We isolated and quantified the influence of hypoxia on
349 chemoresistance, as measured by IC50 values, when cells were cultured in 3D with normal liver
350 stiffness (4 mg/ml) and in 2D monolayers both under hypoxic conditions. Overall, the introduction of
351 hypoxic conditions to 2D monolayers or 3D collagen hydrogels with normal stiffness (4 mg/ml)
352 showed a change in response between the HCC cell lines for 24-hour treatment durations and saw
353 minimal changes for 48-hour treatment durations as shown in Figure S-III. Hypoxia consistently
354 increased IC50 values of doxorubicin against HepG2 cells but decreased IC50 values of doxorubicin
355 against C3Asub28 IC50 compared to normoxic conditions for all stiffnesses. The response of HuH-7
356 and Hep3B2 cells to doxorubicin under hypoxia was variable depending on if they were cultured in 2D
357 or 3D.

358 We next isolated the impact that hypoxia plays in the regulation of chemoresistance of different HCC
359 cell lines in 3D microenvironments. We first analyzed the effect that the shift from 4 mg/mL to 7
360 mg/mL collagen concentration had on doxorubicin IC50 values under hypoxic (1% O_2) conditions and
361 then quantified the impact that the shift from normoxia to hypoxia had within each collagen
362 concentration. Within both normal (4 mg/mL) and cirrhotic (7 mg/mL) liver stiffness, the introduction
363 of hypoxia resulted in a general increase in doxorubicin IC50 values, except for C3Asub28 which
364 shows the opposite trend. However, we did not observe a statistical significance of doxorubicin IC50

This is a provisional file, not the final typeset article

365 values when Hep3B2 cells cultures in 3D normal-hypoxic or 3D cirrhotic-hypoxic conditions relative
366 to their normoxic counterparts. All of the observed trends in IC50 fold changes suggested that HCC
367 cells, depending on the underlying phenotype (denoted by the different HCC cell lines utilized), can
368 display a differential change in IC50 values of doxorubicin dependent upon microenvironmental
369 stiffness and oxygen availability.

370 3.6 Matrix Stiffness and Hypoxia Modulate Cell Viability in Response to Sorafenib 371 Treatment in Hepatic 3D Cultures

372 Sorafenib is not primarily utilized to induce direct cell death, its mechanism is to inhibit kinases
373 responsible for promoting angiogenesis and cell growth, mainly VEGFR, PDGFR, and RAF[15]. As
374 such, even high doses are not sufficient to terminate 50% of the HCC population rendering the
375 calculation of IC50 values impossible. We investigated the direct cytotoxic impact of sorafenib to
376 establish baseline values for more clinically relevant combined therapeutic administration of sorafenib
377 and doxorubicin. Clinically relevant standard (11 μM) and high (22 μM) doses of sorafenib reported
378 in previous studies were tested on four different HCC cell lines [42]. We observed many of the same
379 trends previously observed for doxorubicin chemoresistance (Figure 3). We note that C3Asub28
380 demonstrated the lowest levels of cell death. We also demonstrate that in C3asub28 cells that an
381 increase in microenvironmental stiffness correlated to a general increase in sorafenib chemoresistance.
382 However, the effects of hypoxia were more varied, and sorafenib chemoresistance differed depending
383 on the cell line, sorafenib dose, and microenvironmental stiffness. In our comparison of sorafenib
384 treated cells in 3D to the untreated 3D controls, we established that cell viability is not significantly
385 impacted at standard, 11 μM, Sorafenib doses for many of the cell lines regardless of matrix stiffness
386 or oxygen concentration at 24-hour treatment durations. However, higher doses of sorafenib, 22 μM,
387 shows a much higher direct cytotoxic effect across all HCC cell lines and microenvironmental
388 conditions tested. The influence of hypoxia on sorafenib chemoresistance has a markedly different
389 dynamic than what we have previously seen with doxorubicin.

390 3.7 Sorafenib Improves Minimum Required Dose of Doxorubicin for Acute Toxicity

391 Combined administration of doxorubicin and sorafenib in HCC patients has been commonly used due
392 to their potential synergistic effect [41,46]. Doxorubicin is used to inhibit tumor proliferation[47], while
393 sorafenib is used to inhibit angiogenesis and tumor cell proliferation in the TME [15]. Cells cultured in
394 3D normal and cirrhotic hydrogels were investigated for the impact of doxorubicin-sorafenib
395 combination therapy to determine how the introduction of sorafenib influenced the resulting cell
396 viability. Cell viability in normal and cirrhotic tissue with a 24-hour treatment duration of both drugs
397 and the influence of hypoxia are presented in Figure 3 and discussed in this section. Treatment efficacy
398 is reported as fold viability change compared to untreated controls reported in Figure S-IV. In addition,
399 we explore how the addition of sorafenib can lower the minimum required doxorubicin dose to produce
400 a significant change in cell viability from untreated controls. For this analysis, statistical comparison
401 ($p<0.05$) of viability under tested doses and untreated samples were compared, and minimum dose to
402 induce cytotoxicity was reported. We found minimal differences between 24- and 48-hour treatments
403 with these drugs and present 48-hour treatment results in Figure S-V.

404 HepG2 cells treated with combination therapy demonstrated a general decrease in the minimum
405 required concentration of doxorubicin to initiate statistically significant cell death compared to the non-
406 drug treated control. Under 3D normal-normoxic conditions, the required minimum doxorubicin dose
407 decreased from 1 μM to 0.5 μM and 0 μM for standard and high doses of sorafenib, respectively.
408 Similarly, 3D cirrhotic-normoxic conditions with sorafenib reduced the minimum doxorubicin dose
409 from 10 μM to 1 μM for both standard and high sorafenib doses. Under hypoxic conditions, we found

410 that the trend held. HepG2 cells in the cirrhotic-hypoxic conditions in combination therapy showed a
411 decreased minimum doxorubicin concentration from 10 μM to 1 μM compared to 3D cirrhotic-
412 normoxic conditions for both standard and high doses of sorafenib. Under normal-hypoxic conditions,
413 the required minimum dose of doxorubicin decreased from 5 μM to 0.5 μM and 0 μM compared to 3D
414 normal-normoxic conditions for standard and high doses of sorafenib, respectively. Although the
415 HepG2 phenotype showed a higher chemoresistance to doxorubicin in hypoxic and cirrhotic culture
416 conditions relative to normoxic and normal, the combination with sorafenib significantly diminished
417 the required dose of doxorubicin to initiate toxicity.

418 The C3Asub28 cell line demonstrated the highest levels of chemoresistance out of all of the selected
419 HCC cell lines, however like all other cell lines, the combination of sorafenib with doxorubicin
420 considerably lowered the required doxorubicin dose required to induce a significant decrease in cell
421 viability compared to samples treated only with doxorubicin. Without sorafenib, 10 μM and 50 μM
422 doxorubicin concentrations were required to initiate tumor cell toxicity for normal-normoxic and
423 cirrhotic-normoxic microenvironments, respectively. Under hypoxia, the required dose of doxorubicin
424 decreased from 50 μM to 5 μM in cirrhotic-hypoxic conditions only. For the normal-hypoxic condition,
425 the minimum required concentration to initiate tumor cell toxicity did not change (5 μM) for the high
426 and standard doses of sorafenib compared to the control. On the other hand, for the cirrhotic-hypoxic
427 condition, doxorubicin effectiveness to initiate tumor cell toxicity improved by 2.82 ($p=0.05$) and
428 19.88-fold ($p=0.04$) for the standard and high doses of sorafenib, respectively compared to samples
429 treated only with doxorubicin. Given that the C3Asub28 cell line required the highest dose of
430 doxorubicin, the combination with sorafenib significantly lowered the required dose of doxorubicin to
431 initiate tumor cell toxicity.

432 HuH-7 cells under the normal-normoxic condition showed a decrease in the minimum required dose
433 of doxorubicin from 0.1 μM to 0.001 μM and 0 μM for a significant decrease in cell viability compared
434 to normal-hypoxic conditions for standard and high doses of sorafenib respectively. Under the
435 cirrhotic-normoxic condition, standard sorafenib dose did not improve the minimum required
436 doxorubicin concentration. However, the high dose of sorafenib (22 μM) improved the minimum
437 required doxorubicin concentration to initiate toxicity from 1 μM to 0.1 μM. For the normal-hypoxic
438 condition, the required minimum dose of doxorubicin to initiate toxicity decreased from 0.5 μM to 0
439 μM for both standard and high doses of sorafenib compared to normal-normoxic conditions. A similar
440 trend was observed or the cirrhotic-hypoxic condition, the minimum required dose of doxorubicin
441 decreased from 0.1 μM to 0 μM for both standard and high doses of sorafenib compared to cirrhotic-
442 normoxic conditions.

443 For Hep3B2 cells, the standard dose of sorafenib (11 μM) under normal-normoxic conditions caused
444 a decrease in the minimum required dose of doxorubicin for a significant decrease ($p=0.05$) in cell
445 viability by 1.33-fold compared to no sorafenib. However, only the high dose of sorafenib (22 μM)
446 treatment of Hep3B2 cells improved the required doxorubicin dose in the cirrhotic-normoxic condition
447 from 0.1 μM to 0 μM. In both normal-hypoxic and cirrhotic-hypoxic conditions, the combined
448 treatment showed an improved minimum doxorubicin concentration from 0.1 μM to 0 μM for both
449 standard and high doses of sorafenib to initiate toxicity in cells.

This is a provisional file, not the final typeset article

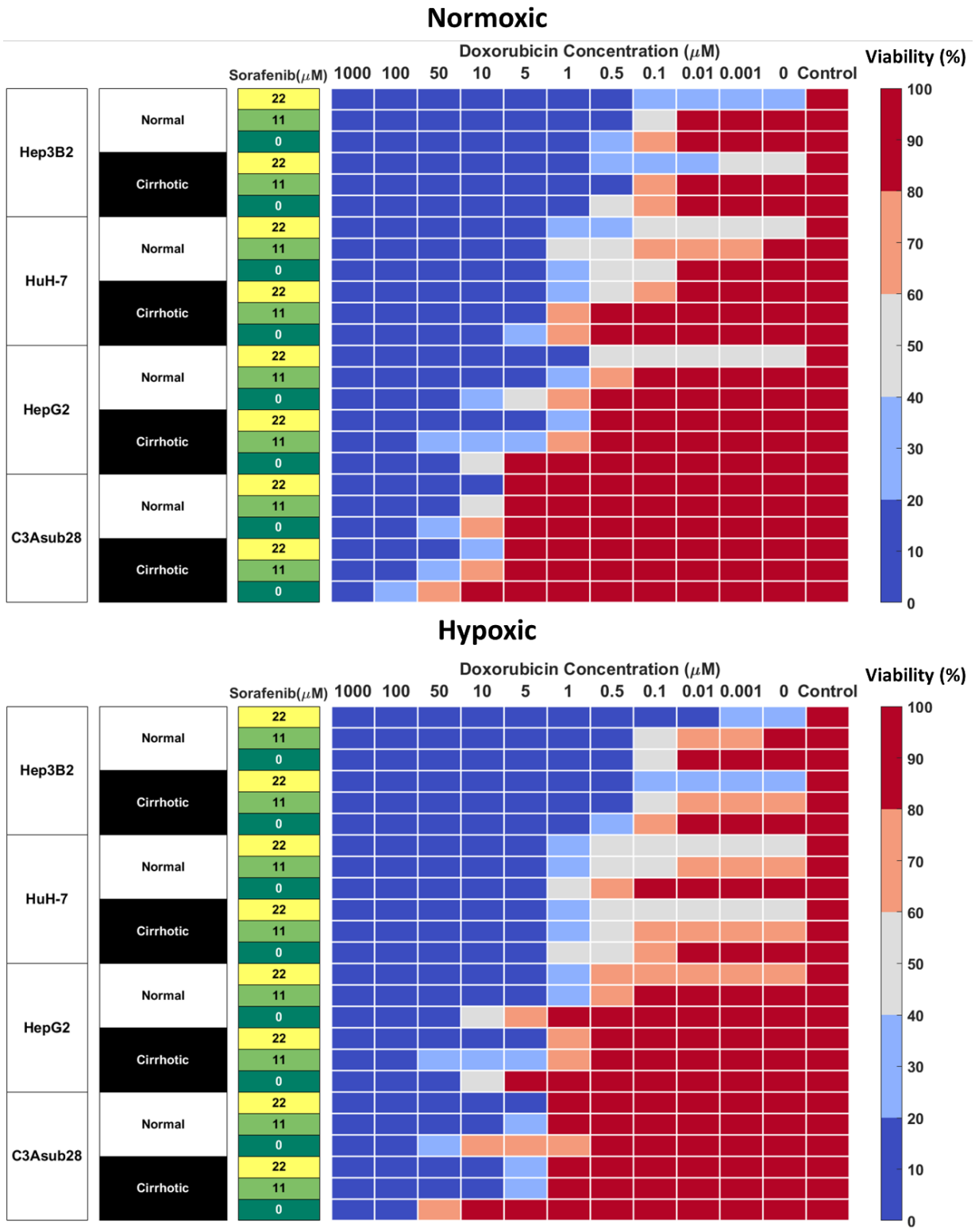

Figure 3: Combined doxorubicin and sorafenib treatment efficacy of HCC cell lines under the influence of hypoxia and cirrhosis. HCC cell types show sensitivity to combined sorafenib and doxorubicin treatment for 24 hours. Cells cultured in 3D normal and cirrhotic hydrogels in hypoxic and normoxic conditions. Cell viability was analyzed and plotted as a percentage of the untreated control. A combination of doxorubicin with sorafenib improves treatment efficacy. The influence of cirrhosis decreased HCC cell death.

457 **3.8 Cirrhosis and Hypoxia Regulated HCC Metabolic Activity**

458 The CYP3A4 enzyme is one of the major mechanisms of drug metabolism for cancer therapeutics,
459 including sorafenib and doxorubicin, in the liver. These enzymes can metabolize drugs before they
460 have the chance to cause their intended direct cytotoxic effects on the cells.[14]. CYP3A4 metabolic
461 activity of the HCC cell lines was measured in 2D monolayers and in 3D collagen I hydrogels in
462 response to different stiffness and hypoxic conditions. Regulation of CYP3A4 by cirrhosis and hypoxia
463 is presented in Figure 4. In agreement with the previously published literature, the C3Asub28 cell line
464 expressed much higher CYP3A4 expression than other HCC cell lines[38]. In our study, C3Asub28
465 CYP3A4 expression is 7.17 ± 2.73 fold higher than the HepG2 cell line, which is within the range of
466 previously published work (6.1 ± 0.2 fold) [38]. The introduction of hypoxia significantly downregulated
467 CYP3A4 expression compared to normoxia in all microenvironments (p=0.03). CYP3A4 expression
468 of C3Asub28 cells did not change with culture in 3D normal-normoxic and 3D normal-hypoxic
469 conditions than similar 2D conditions (p=0.78).

470 On the other hand, 3D cirrhotic-normoxic and cirrhotic-hypoxic culture upregulated CYP3A4
471 expression by 1.50 (p=0.007) and 1.65 (p=0.01) fold compared to 3D normal-normoxic and normal-
472 hypoxic conditions, respectively. HepG2 cell lines expressed significantly lower (p=0.02) CYP3A4
473 expression compared to the C3Asub28 cell line. However, unlike the C3Asub28 cell line, hypoxia
474 upregulated CYP3A4 expression in HepG2 cell lines compared to normoxia for both 2D and 3D
475 microenvironments (p=0.04). 3D normal-normoxic and normal-hypoxic culture upregulated CYP3A4
476 expression compared to 2D normoxic and 2D hypoxic culture by 1.90 (p=0.03) and 1.35 (p=0.003)
477 fold, respectively. Similarly, 3D cirrhotic-normoxic and cirrhotic-hypoxic culture upregulated
478 CYP3A4 expression compared to 3D normal-normoxic and normal-hypoxic stiffness by 2.13
479 (p=0.004) and 2.00 (p=0.0002) fold, respectively. HuH-7 cells expressed relatively lower values of
480 CYP3A4, and none was detected in 3D culture conditions. Furthermore, the Hep3B2 cell line did not
481 express any CYP3A4 expression in all culture conditions. These results show that HCC cells express
482 different basal levels of CYP3A4 and that this expression is can be directly regulated by TME oxygen
483 concentration and stiffness.

This is a provisional file, not the final typeset article

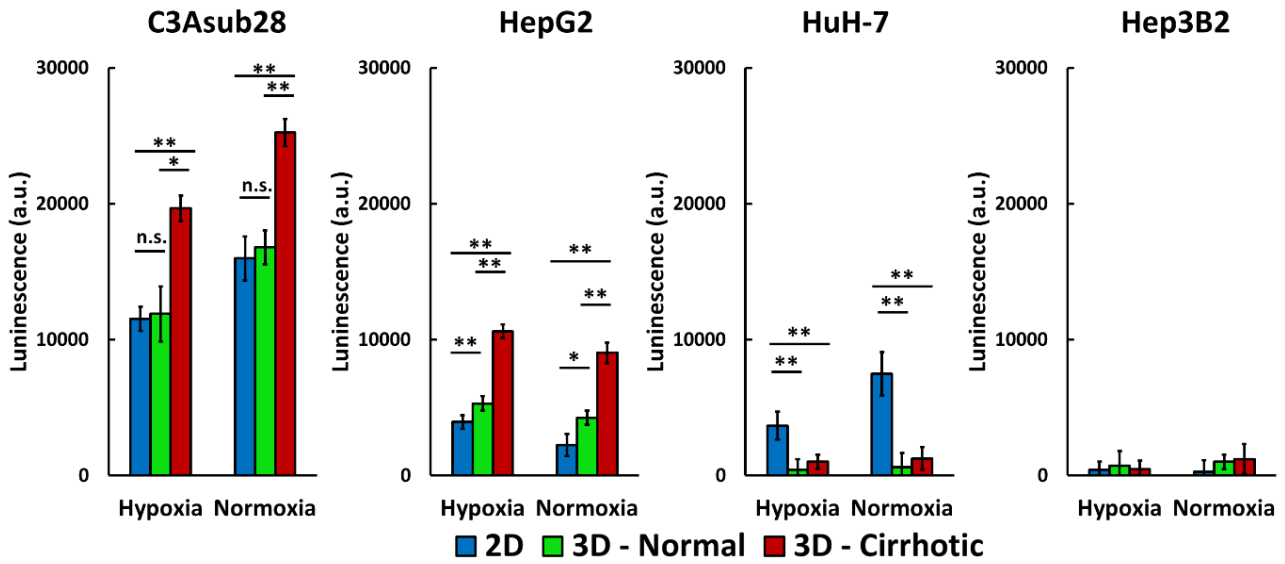

Figure 4: Regulation of CYP3A4 is responsible for drug metabolization by HCC cell lines in response to hypoxic and cirrhotic conditions. Presence of cirrhosis and hypoxia altered CYP3A4 activity differently between HCC cell lines. Data represented as mean ± standard deviation. * denotes significance for cirrhotic and normal 3D samples compared to the 2D monolayer. * $p < 0.05$, ** $p < 0.01$.

4 Discussion

In this study, we establish that chemoresistance can be regulated by hypoxic and cirrhotic conditions in the TME through direct modulation of CYP3A4 expression. This regulation can differentially alter the efficacy of chemotherapeutic drugs in HCC cell lines, which potentially has clinical translation to patient-specific HCC treatments. We examined the direct impact of TME stiffness and oxygen concentration, variables commonly associated with HCC tumors on cellular response to chemotherapeutics. This impact was measured by determining the difference in cell viability in response to chemotherapeutic treatment and regulation of the expression of the primary drug-metabolizing enzyme CYP3A4. Using a collagen-based hydrogel system, we observed that 3D culture alone significantly modulates resistance to doxorubicin and sorafenib in HepG2, C3Asub28, and HuH-7 cells but not for Hep3B2 cells. This stiffness-dependent resistance was not observed in similar Hep3B2 cultures, which warrants further investigation into potential phenotypic and genotypic differences in this specific cell line that might elucidate this response. This differential regulation of chemoresistance in different cell lines of the same cancer type is not unique to HCC. This phenomenon has also been observed in other cancers: The chemoresistance indicator, ethoxyresorufin, was upregulated in 3D culture conditions compared to 2D culture in the C3A cell line. This is in agreement with HepG2 and C3Asub28 doxorubicin treatment findings [48]. Equivalently, the IC50 of C3A cells after treatment with paracetamol, trovafloxacin, and fialuridine were found to be higher in 2D culture conditions compared to 3D culture conditions. This result corresponds with our HuH-7 and Hep3B2 doxorubicin chemoresistance findings [24]. Overall, these studies suggest that drug efficacy in 2D vs. 3D conditions depends on cell phenotype and drug type. This coincides with our findings in which HepG2 and C3Asub28 cell lines had greater chemoresistance in 3D culture compared to 2D but showed the converse trend for HuH-7 and Hep3B2 cells.

Cirrhosis and desmoplastic stiffening in the TME has been shown to be potential factors regulating drug chemoresistance [49]. In our study, HepG2 chemoresistance to sorafenib and doxorubicin increased

515 in response to cirrhotic stiffness relative to their culture in a matrix of normal stiffness. The C3Asub28
516 cell line demonstrated a higher chemoresistance to doxorubicin in response to cirrhotic conditions than
517 other tested HCC cells. Similar to the HepG2 cell line, a rise in stiffness also increased the
518 chemoresistance to doxorubicin of the C3Asub28 cell line. However, sorafenib alone did not alter the
519 cell viability of the C3Asub28 cell line for the considered doses potentially attributed to the cell line's
520 high baseline CYP3A4 metabolic activity. The resistance of HuH-7 and Hep3B2 cells to doxorubicin
521 was not altered in response to cirrhosis, whereas CYP3A4 expression of these cell lines did not change
522 in response to cirrhosis. However, the same cell lines were shown to have higher chemoresistance to
523 sorafenib in response to cirrhosis. Although CYP3A4 carries out the majority of metabolic activity in
524 hepatocytes, other minor cytochromes, such as CYP1A2, 2A6, 1A2, and 2C9, exist and may also alter
525 the drug chemoresistance to an as yet unknown extent. The additional CYP expression present in HCC
526 cells may be responsible for the differential effect of cirrhosis on chemoresistance differences between
527 sorafenib and doxorubicin [50]. Furthermore, studies in literature showed that a rise in stiffness does not
528 always increase the chemoresistance of cancer cells [49]. The increase in TME stiffness may improve
529 IC50 of MDA-MB-231 triple-negative breast cancer cells to doxorubicin [27]. However, the same study
530 showed that MCF-7 HER2+ breast cancer cells did not show a stiffness-dependent resistance to
531 doxorubicin. This study hypothesized the increase of stiffness altered chemoresistance differently
532 because MCF-7 remained in an epithelial phenotype, but MDA-MB-231 had a mesenchymal
533 phenotype. Similarly, stiffness induces chemoresistance of BxPC-3 and Suit2-007 pancreatic cancer
534 cells to paclitaxel, but not to gemcitabine [51]. These studies hypothesized the differential effect of
535 chemoresistance to different drugs between cell lines could be related to phenotypical differentiation
536 from epithelial to mesenchymal phenotype. In addition, HepG2, HuH-7, and Hep3B2 cell lines have
537 different phenotypic profiles and differentiation levels, potentially explaining differences in their
538 chemoresistance and metabolic activity in response to cirrhosis [52].

539 Hypoxia is known to be one of the regulating factors of chemoresistance [53]. In our study, HepG2
540 chemoresistance to doxorubicin and sorafenib increased in response to hypoxia compared to the
541 normoxic condition as measured both by increased IC50 values and CYP3A4 expression. However,
542 for C3Asub28 and HuH-7, chemoresistance decreased in response to hypoxia compared to normoxia.
543 Previous studies have also demonstrated the differential effect of hypoxia on drug efficacy, depending
544 on the cell line and phenotype. The presence of hypoxia has been shown to upregulate hypoxia-induced
545 factor (HIF1-α), but this alters the CYP isoforms differently in various medulloblastoma cell lines [54].
546 The molecular pathway still could not be explained in this study, but it has been hypothesized that
547 nuclear receptors, namely PPARα, PPARγ, or ER-α, as well as the constitutive androstane and
548 pregnane X receptors, have found to be altered differently under hypoxia [54]. In addition to this,
549 chemoresistance does not always increase in response to hypoxia [53]. The same study also showed the
550 regulation of chemoresistance under hypoxia is not universal between ovarian, renal, breast, lung, and
551 lymphoma cancer cell lines and varies for different drugs. This supports our data showing the
552 differential effects of hypoxia on doxorubicin IC50 values of the tested HCC cell lines [53]. Also, hypoxia
553 increases HepG2 chemoresistance to doxorubicin, in confirmation with our study, but not to rapamycin
554 [23]. In parallel to this, a significant decrease in apoptotic cells induced by cisplatin was reported under
555 hypoxic conditions for HepG2 and MHCC97L cell lines, which is in agreement with what we observed
556 with increased chemoresistance of HepG2 cells under hypoxic conditions [55]. It has also been showed
557 that hypoxia downregulates drug-metabolizing enzymes and subsequently the chemoresistance of the
558 HepaRG hepatoma cell line, which agrees with our findings of C3Asub28 CYP3A4 modulation under
559 hypoxia [56].

560 Consequently, the differential role of hypoxia on molecular chemoresistance expressions and drug
561 efficacy has been reported. It has been shown that HIF1-α is upregulated due to a lack of oxygen in

This is a provisional file, not the final typeset article

562 TME. This may or may not induce drug transporters such as MDR1 and targets of delivered drugs
563 (topoisomerase II) in each cell line [20]. Additionally, possible nuclear receptors have been proposed to
564 regulate CYP3A4 in response to hypoxia through the expression of HIF1-α and p53 expression[57].
565 Alternation of molecular drug transport mechanisms could be the reason why we observed variable
566 chemoresistance between different HCC cell lines under hypoxia.

567 Our study showed CYP3A4 expression is regulated by microenvironment stiffness and hypoxia for
568 HepG2, C3Asub28, and HuH-7 cell lines providing a potential mechanism connecting the TME to the
569 chemotherapeutic response. The regulation of CYP3A4 resulted in a significant impact on the efficacy
570 of doxorubicin and sorafenib, whose trends in the regulation mirror the observed changes in cell
571 viability in response to the drugs. Doxorubicin IC50 was higher, and sorafenib terminated less HCC
572 population for HepG2 and C3Asub28 cells in cirrhotic, 7 mg/ml, microenvironments in general
573 compared to healthy, 4 mg/mL, stiffness reflecting the CYP3A4 expression in those
574 microenvironments. However, we did not see any significant IC50 change in response to doxorubicin
575 for the HuH-7 cell line when cultured in normal and cirrhotic 3D microenvironments. In addition,
576 CYP3A4 expression of HuH-7 did not change when cultured in normal and cirrhotic 3D
577 microenvironments, which is parallel with IC50 findings.

578 Moreover, in general, we demonstrate that hypoxia increases doxorubicin IC50 against HepG2 cells
579 but C3Asub28 cells. The change of doxorubicin IC50 was parallel to the regulation of CYP3A4
580 expression. Hypoxia upregulated CYP3A4 expression of HepG2 cells but downregulated CYP3A4
581 expression of C3Asub28 cells. This work further confirms the upregulated metabolic expression of
582 CYP3A4 decreases doxorubicin efficacy in confirmation with previous studies across multiple cancer
583 types, including liver[58], colorectal[29], breast[59], and prostate[60]. Inhibition of CYP3A4 activity of human
584 primary hepatocytes has shown to suppress human pregnane X receptor (hPXR) agonist-induced
585 chemoresistance [61]. Overexpression of CYP3A4 in tumor tissues and chemoresistance to therapeutics
586 has been shown in clinical practices [62]. Similarly, there is evidence that therapeutic efficacy of drugs
587 have been diminished through CYP3A4 enzyme expressed by hepatocellular carcinoma cells[63]. These
588 studies agree with our findings on the regulation of chemoresistance based on CYP3A4 activity.
589 However, our work presents the significant finding that the regulation of CYP3A4 expression can be
590 directly tied to the tumor microenvironment. We demonstrate that CYP3A4 activity can be regulated
591 by oxygen concentration and TME stiffness, subsequently altering the metabolism of the
592 chemotherapeutic drugs in HCC cell lines. Possible nuclear receptor pathways regulating CYP3A4 in
593 response to hypoxia through HIF1-α, p53, PPARα, VDR, FXR, and LXR have been proposed and
594 hypothesized that hypoxia could affect CYP3A4 at different degrees [57]. Furthermore, TME stiffness
595 has been hypothesized to alter CYP3A4 differentially through yes-associated protein (YAP) pathway
596 [64]. This likely has a direct clinical translation to *in vivo* HCC regulation enforced by the clinical
597 observations of highly variable patient to patient HCC CYP3A4 expression [65]. The majority of the
598 current HCC treatments result in poor treatment outcomes, as such, the consideration of tumor
599 microenvironment properties (such as stiffness variation due to the changing fibrosis scores of patients,
600 presence of different levels of hypoxia as a result of this desmoplastic stiffening in the TME), and CYP
601 expression levels could potentially bring benefits to outcomes of HCC treatment, and provide a basis
602 for personalized HCC treatment [62,66].

603 Overall, this work demonstrates TME stiffness and oxygen concentration modulates CYP3A4
604 expression of HCC cells and, consequently, their chemoresistance to doxorubicin and sorafenib
605 treatment. We determined the existence of a stiffness-dependent resistance to doxorubicin and
606 sorafenib, depending on the differential genetics of the HCC, such as phenotypical changes from
607 epithelial to mesenchymal [27]. HepG2 and C3Asub28 cells showed a higher chemoresistance to

608 doxorubicin and sorafenib under cirrhotic conditions. Conversely, we did not observe a change in
609 chemoresistance for HuH-7 and Hep3B2 cell lines to doxorubicin in response to cirrhotic conditions,
610 which may be due to underlying genotypic differences including differentiation levels, which alter
611 metabolism pathways through glucose, glutamine, and glutamate [52]. Hypoxia demonstrated a much
612 different impact on the HCC cells, upregulating the chemoresistance of HepG2 and HuH-7, but
613 downregulating chemoresistance of the C3Asub28 cell line. We did not observe a significant variation
614 of chemoresistance in the Hep3B2 cell line in 3D culture. Drug metabolism, measured by CYP3A4
615 expression, mirrored effective chemoresistance measured by IC50 values in cell vitality assays. We
616 saw an increase in CYP3A4 expression in the 3D culture of C3Asub28 and HepG2 cell lines compared
617 to 2D, but this expression decreased for the HuH-7 cell line for both hypoxic and normoxic conditions.
618 At a minimum, the presence of a 3D culture system significantly modulates the response of HCC to
619 chemotherapy over the standard 2D methods. Previously it has been shown 3D culture alters the
620 integrin ligands (such as AKT and RAF), which are the targeting for doxorubicin and sorafenib,
621 differently among different cell lines compared to 2D culture [49].

622 Further, the stiffness of the microenvironment, seen in HCC patients with cirrhosis, modulates drug
623 resistance and should be taken into consideration when determining treatment options and doses. While
624 CYP3A4 maintains the majority of the drug metabolism in the liver, other enzymes such as CYP2A6,
625 1A2, and 2C9 has shown to have a minor contribution to drug metabolism [62], and provide further
626 insight in IC50 of Hep3B2 variation we observed between 2D and 3D microenvironments but not
627 captured a difference in CYP3A4 expression. Further expansion of this work is needed to investigate
628 the varied response between existing HCC lines or patient-specific primary tumor cells that might
629 provide insight into the known differential effectiveness of standard HCC treatments *in vivo* [66].
630 Potentially, other drugs used to treat HCC in clinical practice such as lenvatinib could be tested in this
631 system to observed its potential effect on HCC treatment [67].

632 **5 Acknowledgment**

633 The authors would like to thank Dr. Wei Li (Department of Mechanical Engineering, the University of
634 Texas at Austin) and Dr. Christopher Sullivan (Department of Molecular Sciences) for generously
635 gifting C3Asub28 cells and HuH-7, respectively. This work was completed with support from the
636 Veterans Health Administration and with resources and the use of facilities at the Central Texas
637 Veterans Health Care System, Temple, Texas. The contents do not represent the views of the U.S.
638 Department of Veterans Affairs or the United States Government. T.E.Y. is a CPRIT scholar in cancer
639 research.

640 **6 Funding**

641 The authors acknowledge the support of the Cancer Prevention Research Institute of Texas (CPRIT)
642 for funding part of this work through grants RR160005, National Cancer Institutes for funding through
643 R21EB019646, R01CA186193, R01CA201127-01A1, U24CA226110 and U01CA174706, National
644 Institute of Diabetes and Digestive and Kidney Diseases funding through awards R01DK082435 and
645 R01DK112803 and Department of Veterans Affairs Biomedical Laboratory Research and
646 Development Service funding through award BX003486.

647 **7 Author contributions**

648 Conceptualization: A.O. and M.N.R. conceived of the idea for the study. Supervision: E.N.K.C, T.E.Y.
649 and M.N.R. supervised the project. E.N.K.C., S.D., M.M., T.E.Y. and M.N.R provided feedback and
650 assistance with manuscript preparation. Investigation: A.O., D.L.S., and M.N.R were responsible for

This is a provisional file, not the final typeset article

651 performing the studies and analyzing the experimental data. Writing: A.O. wrote the initial draft of the
652 paper. All authors discussed the results and revised the manuscript.

653 **8 References**

654 1. Grandhi MS, Kim AK, Ronnekleiv-Kelly SM, Kamel IR, Ghasebeh MA, Pawlik TM.
655 Hepatocellular carcinoma: From diagnosis to treatment. *Surg Oncol*. 2016;25(2):74-85.
656 doi:10.1016/j.suronc.2016.03.002

657 2. Petrick JL, Kelly SP, Altekruse SF, McGlynn KA, Rosenberg PS. Future of hepatocellular
658 carcinoma incidence in the United States forecast through 2030. *J Clin Oncol*.
659 2016;34(15):1787-1794. doi:10.1200/JCO.2015.64.7412

660 3. Siegel RL, Miller KD, Jemal A. Cancer Statistics, 2018. *CA CANCER J CLIN*. 2018;68(1):7-
661 30. doi:10.3322/caac.21387

662 4. Davis GL, Dempster J, Meler JD, et al. *Hepatocellular Carcinoma: Management of an*
663 *Increasingly Common Problem*. Vol 21.; 2008. doi:10.1080/08998280.2008.11928410

664 5. Marrero JA, Kulik LM, Sirlin CB, et al. Diagnosis, Staging, and Management of Hepatocellular
665 Carcinoma: 2018 Practice Guidance by the American Association for the Study of Liver
666 Diseases. *Hepatology*. 2018;68(2):723-750. doi:10.1002/hep.29913

667 6. Abou-Alfa GK, Niedzwieski D, Knox JJ, et al. Phase III randomized study of sorafenib plus
668 doxorubicin versus sorafenib in patients with advanced hepatocellular carcinoma (HCC):
669 CALGB 80802. *J Clin Oncol*. 2016;34:192-192. doi:10.1200/jco.2016.34.4_suppl.192

670 7. Grazie LM. et al. Chemotherapy for hepatocellular carcinoma: The present and the future, *World*
671 *J Hepatol*. 2017;9(21):9-21.

672 8. Lohitesh K, Chowdhury R, Mukherjee S. Resistance a major hindrance to chemotherapy in
673 hepatocellular carcinoma: An insight. *Cancer Cell Int*. 2018;18(1):44. doi:10.1186/s12935-018-
674 0538-7

675 9. LU L-C, CHEN P-J, YEH Y-C, et al. Prescription Patterns of Sorafenib and Outcomes of
676 Patients with Advanced Hepatocellular Carcinoma: A National Population Study. *Anticancer*
677 *Res*. 2017;37(5):2593-2599. doi:10.21873/anticanres.11604

678 10. Llovet JM, Ricci S, Mazzaferro V, et al. Sorafenib in advanced hepatocellular carcinoma. *N*
679 *Engl J Med*. 2008;359(4):378-390. doi:10.1056/NEJMoa0708857

680 11. Schicho A, Hellerbrand C, Krüger K, et al. Impact of Different Embolic Agents for Transarterial
681 Chemoembolization (TACE) Procedures on Systemic Vascular Endothelial Growth Factor
682 (VEGF) Levels. *J Clin Transl Hepatol*. 2016;4(4):288-292. doi:10.14218/jcth.2016.00058

683 12. Marin HL, Furth EE, Olthoff K, Shaked A, Soulen MC. Histopathologic outcome of neoadjuvant
684 image-guided therapy of hepatocellular carcinoma. *J Gastrointest Liver Dis*. 2009;18(2):169-
685 176. Accessed June 11, 2019.

686 13. De Montellano PRO. Cytochrome P450-activated prodrugs. *Future Med Chem*. 2013;5(2):213-

687 228. doi:10.4155/fmc.12.197

688 14. Rodriguez-Antona C, Ingelman-Sundberg M. Cytochrome P450 pharmacogenetics and cancer.
689 *Oncogene*. 2006;25(11):1679-1691. doi:10.1038/sj.onc.1209377

690 15. Keating GM, Santoro A. *Sorafenib: A Review of Its Use in Advanced Hepatocellular*
691 *Carcinoma*. Vol 69.; 2009. doi:10.2165/00003495-200969020-00006

692 16. Xu W, Zhang X, Yu J, et al. Targeting the vasculature in hepatocellular carcinoma treatment:
693 Starving versus normalizing blood supply. *Clin Transl Gastroenterol*. 2017;8(6):e98.
694 doi:10.1038/ctg.2017.28

695 17. Lencioni R, Petruzzi P, Crocetti L. Chemoembolization of hepatocellular carcinoma. *Semin*
696 *Intervent Radiol*. 2013;30(1):3-11. doi:10.1055/s-0033-1333648

697 18. Koyama Y, Brenner DA. Liver inflammation and fibrosis. *J Clin Invest*. 2017;127(1):55-64.
698 doi:10.1172/JCI88881

699 19. Affo S, Yu L-X, Schwabe RF. The Role of Cancer-Associated Fibroblasts and Fibrosisin Liver
700 Cancer. *Annu Rev Pathol Mech Dis*. 2016;12(1):153-186. doi:10.1146/annurev-pathol-052016-
701 100322

702 20. Doktorova H, Hrabeta J, Khalil MA, Eckschlager T. Hypoxia-induced chemoresistance in
703 cancer cells: The role of not only HIF-1. *Biomed Pap*. 2015;159(2):166-177.
704 doi:10.5507/bp.2015.025

705 21. Beckwitt CH, Clark AM, Wheeler S, et al. Liver 'organ on a chip.' *Exp Cell Res*.
706 2018;363(1):15-25. doi:10.1016/j.yexcr.2017.12.023

707 22. Rodríguez-Antona C, Leskelä S, Zajac M, et al. Expression of CYP3A4 as a predictor of
708 response to chemotherapy in peripheral T-cell lymphomas. *Blood*. 2007;110(9):3345-3351.
709 doi:10.1182/blood-2007-02-075036

710 23. Bowyer C, Lewis AL, Lloyd AW, Phillips GJ, MacFarlane WM. Hypoxia as a target for drug
711 combination therapy of liver cancer. *Anticancer Drugs*. 2017;28(7):771-780.
712 doi:10.1097/CAD.0000000000000516

713 24. Webb SD, Colley HE, Sharma P, Murdoch C, Gaskell H, Williams DP. Characterization of a
714 functional C3A liver spheroid model. *Toxicol Res*. 2016;5(4):1053-1065.
715 doi:10.1039/c6tx00101g

716 25. Khawar IA, Park JK, Jung ES, Lee MA, Chang S, Kuh HJ. Three Dimensional Mixed-Cell
717 Spheroids Mimic Stroma-Mediated Chemoresistance and Invasive Migration in hepatocellular
718 carcinoma. *Neoplasia*. 2018;20(8):800-812. doi:10.1016/j.neo.2018.05.008

719 26. Antoine EE, Vlachos PP, Rylander MN. Tunable collagen I hydrogels for engineered
720 physiological tissue micro-environments. *PLoS One*. 2015;10(3).
721 doi:10.1371/journal.pone.0122500

722 27. Brock A, Joyce MH, Suggs LJ, et al. Phenotypic Basis for Matrix Stiffness-Dependent

This is a provisional file, not the final typeset article

723 Chemoresistance of Breast Cancer Cells to Doxorubicin. *Front Oncol*. 2018;8:337.
724 doi:10.3389/fonc.2018.00337

725 28. Ma L, Barker J, Zhou C, et al. Towards personalized medicine with a three-dimensional micro-
726 scale perfusion-based two-chamber tissue model system. *Biomaterials*. 2012;33(17):4353-4361.
727 doi:10.1016/j.biomaterials.2012.02.054

728 29. Kim HJ, Ingber DE. Gut-on-a-Chip microenvironment induces human intestinal cells to undergo
729 villus differentiation. *Integr Biol*. 2013;5(9):1130-1140. doi:10.1039/c3ib40126j

730 30. Malinen MM, Kanninen LK, Corlu A, et al. Differentiation of liver progenitor cell line to
731 functional organotypic cultures in 3D nanofibrillar cellulose and hyaluronan-gelatin hydrogels.
732 *Biomaterials*. 2014;35(19):5110-5121. doi:10.1016/j.biomaterials.2014.03.020

733 31. Kim JW, Ho WJ, Wu BM. *The Role of the 3D Environment in Hypoxia-Induced Drug and*
734 *Apoptosis Resistance*. Vol 31.; 2011.

735 32. Musah-Eroje A, Watson S. A novel 3D in vitro model of glioblastoma reveals resistance to
736 temozolomide which was potentiated by hypoxia. *J Neurooncol*. 2019;142(2):231-240.
737 doi:10.1007/s11060-019-03107-0

738 33. Adriani G, Pavesi A, Kamm RD. Studying TCR T cell anti-tumor activity in a microfluidic
739 intrahepatic tumor model. In: *Methods in Cell Biology*. Vol 146. ; 2018:199-214.
740 doi:10.1016/bs.mcb.2018.05.009

741 34. Ahn J, Ahn J, Yoon S, Nam YS, Son M, Oh J. Human three-dimensional in vitro model of
742 hepatic zonation to predict zonal hepatotoxicity. *J Biol Eng*. 2019;5:1-15. doi:10.1186/s13036-
743 019-0148-5

744 35. Özkan A, Stolley D, Cressman ENK, et al. The Influence of Chronic Liver Diseases on Hepatic
745 Vasculature: A Liver-on-a-chip Review. *Micromachines*. 2020;11(5):487.
746 doi:10.3390/mi11050487

747 36. Stolley DL, Crouch AC, Özkan A, et al. Combining chemistry and engineering for
748 hepatocellular carcinoma: Nano-scale and smaller therapies. *Pharmaceutics*. 2020;12(12):1-18.
749 doi:10.3390/pharmaceutics12121243

750 37. Ozkan A, Ghousifam N, Hoopes PJ, Yankeelov TE, Rylander MN. In vitro vascularized liver
751 and tumor tissue microenvironments on a chip for dynamic determination of nanoparticle
752 transport and toxicity. *Biotechnol Bioeng*. 2019;116(5):1201-1219. doi:10.1002/bit.26919

753 38. Küblbeck J, Reinisalo M, Mustonen R, Honkakoski P. Up-regulation of CYP expression in
754 hepatoma cells stably transfected by chimeric nuclear receptors. *Eur J Pharm Sci*.
755 2010;40(4):263-272. doi:10.1016/j.ejps.2010.03.022

756 39. Hientz K, Mohr A, Bhakta-Guha D, Efferth T. *The Role of P53 in Cancer Drug Resistance and*
757 *Targeted Chemotherapy*. Vol 8.; 2017. doi:10.18632/oncotarget.13475

758 40. Godugu C, Patel AR, Desai U, Andey T, Sams A, Singh M. AlgiMatrix^{TM} Based 3D Cell Culture
759 System as an In-Vitro Tumor Model for Anticancer Studies. *PLoS One*. 2013;8(1).

760 doi:10.1371/journal.pone.0053708

761 41. Abou-Alfa GK, Shi Q, Knox JJ, et al. Assessment of Treatment with Sorafenib Plus Doxorubicin
762 vs Sorafenib Alone in Patients with Advanced Hepatocellular Carcinoma: Phase 3 CALGB
763 80802 Randomized Clinical Trial. *JAMA Oncol*. 2019;5(11):1582-1588.
764 doi:10.1001/jamaoncol.2019.2792

765 42. Coriat R, Nicco C, Chereau C, et al. Sorafenib-induced hepatocellular carcinoma cell death
766 depends on reactive oxygen species production in vitro and in vivo. *Mol Cancer Ther*.
767 2012;11(10):2284-2293. doi:10.1158/1535-7163.MCT-12-0093

768 43. Hey-Chi Hsu, Wen-Chun Yeh, Pei-Ming Yang, et al. Young's modulus measurements of human
769 liver and correlation with pathological findings. In: *2001 IEEE Ultrasonics Symposium.*
770 *Proceedings. An International Symposium (Cat. No.01CH37263)*. Vol 2. IEEE; 2002:1233-
771 1236. doi:10.1109/ultsym.2001.991942

772 44. Yeh WC, Li PC, Jeng YM, et al. Elastic modulus measurements of human liver and correlation
773 with pathology. *Ultrasound Med Biol*. 2002;28(4):467-474. doi:10.1016/S0301-
774 5629(02)00489-1

775 45. Ozcelikkale A, Shin K, Noe-Kim V, et al. Differential response to doxorubicin in breast cancer
776 subtypes simulated by a microfluidic tumor model. *J Control Release*. 2017;266:129-139.
777 doi:10.1016/j.jconrel.2017.09.024

778 46. Merle P, Blanc JF, Phelip JM, et al. Doxorubicin-loaded nanoparticles for patients with
779 advanced hepatocellular carcinoma after sorafenib treatment failure (RELIVE): a phase 3
780 randomised controlled trial. *Lancet Gastroenterol Hepatol*. 2019;4(6):454-465.
781 doi:10.1016/S2468-1253(19)30040-8

782 47. Cox J, Weinman S. Mechanisms of doxorubicin resistance in hepatocellular carcinoma. *Hepatic*
783 *Oncol*. 2015;3(1):57-59. doi:10.2217/hep.15.41

784 48. Amitay-Shaprut S, Cohen S, Elkayam T, Dvir-Ginzberg M, Harel T. Enhancing the Drug
785 Metabolism Activities of C3A— A Human Hepatocyte Cell Line—By Tissue Engineering
786 Within Alginate Scaffolds. *Tissue Eng*. 2006;12(5):1357-1368. doi:10.1089/ten.2006.12.1357

787 49. Shin JW, Mooney DJ. Extracellular matrix stiffness causes systematic variations in proliferation
788 and chemosensitivity in myeloid leukemias. *Proc Natl Acad Sci U S A*. 2016;113(43):12126-
789 12131. doi:10.1073/pnas.1611338113

790 50. Ashida R, Okamura Y, Ohshima K, et al. CYP3A4 Gene Is a Novel Biomarker for Predicting a
791 Poor Prognosis in Hepatocellular Carcinoma. *Cancer Genomics Proteomics*. 2017;14(6):445-
792 453. doi:10.21873/cgp.20054

793 51. Rice AJ, Cortes E, Lachowski D, et al. Matrix stiffness induces epithelial-mesenchymal
794 transition and promotes chemoresistance in pancreatic cancer cells. *Oncogenesis*.
795 2017;6(7):352. doi:10.1038/oncsis.2017.54

796 52. Nwosu ZC, Battello N, Rothley M, et al. Liver cancer cell lines distinctly mimic the metabolic
797 gene expression pattern of the corresponding human tumours. *J Exp Clin Cancer Res*.

This is a provisional file, not the final typeset article

798 2018;37(1). doi:10.1186/s13046-018-0872-6

799 53. Strese S, Fryknäs M, Larsson R, Gullbo J. *Effects of Hypoxia on Human Cancer Cell Line*
800 *Chemosensitivity*. Vol 13.; 2013. doi:10.1186/1471-2407-13-331

801 54. Valencia-Cervantes J, Huerta-Yepez S, Aquino-Jarquin G, et al. Hypoxia increases
802 chemoresistance in human medulloblastoma DAOY cells via hypoxia-inducible factor 1α-
803 mediated downregulation of the CYP2B6, CYP3A4 and CYP3A5 enzymes and inhibition of
804 cell proliferation. *Oncol Rep*. 2019;41(1):178-190. doi:10.3892/or.2018.6790

805 55. Chi KL, Zhen FY, Ho DW, et al. An Akt/hypoxia-inducible factor-1α/platelet-derived growth
806 factor-BB autocrine loop mediates hypoxia-induced chemoresistance in liver cancer cells and
807 tumorigenic hepatic progenitor cells. *Clin Cancer Res*. 2009;15(10):3462-3471.
808 doi:10.1158/1078-0432.CCR-08-2127

809 56. Boudjema K, Ishida S, Hori T, et al. Drug-metabolising enzymes are down-regulated by hypoxia
810 in differentiated human hepatoma HepaRG cells: HIF-1α involvement in CYP3A4 repression.
811 *Eur J Cancer*. 2009;45(16):2882-2892. doi:10.1016/j.ejca.2009.07.010

812 57. Yuan X, Lu H, Zhao A, Ding Y, Min Q, Wang R. Transcriptional regulation of CYP3A4 by
813 nuclear receptors in human hepatocytes under hypoxia. *Drug Metab Rev*. 2020;0(0):1-10.
814 doi:10.1080/03602532.2020.1733004

815 58. Zhou F, Lu L, Peng X, et al. Sorafenib Metabolism Is Significantly Altered in the Liver Tumor
816 Tissue of Hepatocellular Carcinoma Patient. *PLoS One*. 2014;9(5):e96664.
817 doi:10.1371/journal.pone.0096664

818 59. Breslin S, O'Driscoll L. *The Relevance of Using 3D Cell Cultures, in Addition to 2D Monolayer*
819 *Cultures, When Evaluating Breast Cancer Drug Sensitivity and Resistance*. Vol 7.; 2016.
820 doi:10.18632/oncotarget.9935

821 60. Chen TC, Sakaki T, Yamamoto K, Kittaka A. The roles of cytochrome P450 enzymes in prostate
822 cancer development and treatment. *Anticancer Res*. 2012;32:291-298.

823 61. Abbott KL, Chaudhury CS, Chandran A, et al. Belinostat, at its clinically relevant
824 concentrations, inhibits rifampicin-induced CYP3A4 and MDR1 gene expressions. *Mol*
825 *Pharmacol*. 2019;95(3):324-334. doi:10.1124/mol.118.114587

826 62. Molina-Ortiz D, Camacho-Carranza R, González-Zamora JF, et al. Differential expression of
827 Cytochrome P450 enzymes in normal and tumor tissues from childhood rhabdomyosarcoma.
828 *PLoS One*. 2014;9(4). doi:10.1371/journal.pone.0093261

829 63. Hu DG, Mackenzie PI, Lu L, Meech R, McKinnon RA. Induction of human UDP-
830 Glucuronosyltransferase 2B7 gene expression by cytotoxic anticancer drugs in liver cancer
831 HepG2 Cells. *Drug Metab Dispos*. 2015;43(5):660-668. doi:10.1124/dmd.114.062380

832 64. Speer JE, Wang Y, Fallon JK, Smith PC, Allbritton NL. Evaluation of human primary intestinal
833 monolayers for drug metabolizing capabilities. *J Biol Eng*. 2019;13(1). doi:10.1186/s13036-
834 019-0212-1

835 65. Yan T, Lu L, Xie C, et al. Severely impaired and dysregulated cytochrome P450 expression and
836 activities in hepatocellular carcinoma: Implications for personalized treatment in patients. *Mol*
837 *Cancer Ther*. 2015;14(12):2874-2886. doi:10.1158/1535-7163.MCT-15-0274

838 66. Rodríguez-Perálvarez M, Luong TV, Andreana L, Meyer T, Dhillon AP, Burroughs AK. A
839 systematic review of microvascular invasion in hepatocellular carcinoma: Diagnostic and
840 prognostic variability. *Ann Surg Oncol*. 2013;20(1):325-339. doi:10.1245/s10434-012-2513-1

841 67. Chang Lee R, Tebbutt N. Systemic treatment of advanced hepatocellular cancer: new hope on
842 the horizon. *Expert Rev Anticancer Ther*. 2019;19(4):343-353.
843 doi:10.1080/14737140.2019.1585245

844

This is a provisional file, not the final typeset article